

INFLUENCE OF 90°-LAYER THICKNESS ON DAMAGE INITIATION AND PROPAGATION IN CFRP CROSS-PLY LAMINATES

Christian Leopold, Sergej Harder, Christina Buggisch, Wilfried V. Liebig, Bodo Fiedler

Institute of Polymer Composites, Technical University Hamburg-Harburg,
Denickestrasse 15, D-21073 Hamburg, Germany
Email: christian.leopold@tuhh.de, sergej.harder@tuhh.de, christina.buggisch@tuhh.de,
wilfried.liebig@tuhh.de, fiedler@tuhh.de
Web Page: <http://www.tuhh.de/kvweb>

Keywords: Micromechanics, Cross-ply, Ply thickness, Finite element method (FEM), Acoustic emission analysis

Abstract

The influence of layer thickness on failure initiation and damage propagation as matrix cracks in the 90°-layers of cross-ply laminates is investigated experimentally and simulated by using FEM. Decreasing the 90°-layer thickness leads to a shift of damage initiation to higher loads. The crack density and the shape of inter fibre failure also depend on the layer thickness. With increasing 90°-layer thickness, the total amount of cracks decreases, whereas the amount of cracks running through the layer thickness and through the whole specimen width increases. Cracks exhibit a faster growth rate and larger crack opening with increasing layer thickness. This case is more severe for initiating delaminations. A reduction of ply thickness in cross-ply laminates increases the resistance against inter-fibre-fracture and thus offer great potential for increased fatigue lifetime.

1. Introduction

The increasing use of fibre-reinforced plastics (FRP) requires a tailored laminate design and exact knowledge about damage initiation and propagation as well as their failure modes. The onset of damage in multidirectional FRPs controlling the design is matrix cracking in the 90°-layers. Failure initiates at defects in the material as cohesion failure in the matrix between the fibres or as adhesion failure at the fibre matrix interface. Matrix cracks propagate through the thickness between both characteristics and may induce further damage such as delaminations between the 90°- and the neighbouring layers. When regarding cross-ply laminate specimens or parts, cracks initiate at free edges, where out-of-plane or interlaminar stresses occur [1, 2], and propagate inward through the layers oriented perpendicular to the loading direction. At these transverse cracks, stress is zero whereas it reaches a maximum in the middle between two cracks so that a stress redistribution to the neighbouring layers takes place. With increasing load, additional cracks occur at the location of the maximum stress and this process continues, until a saturation is reached at which the maximum stress between two cracks is lower than the transverse strength of the layer. In this case the minimum distance between two cracks is reached [3].

The 90°-ply thickness of a laminate influences the strain at damage onset and the crack propagation within the laminate. Experimental investigations by Parvizi et al. [4, 5] showed that transverse cracking in the 90°-layer of glass fibre reinforced plastic (GFRP) cross-ply laminates is constrained at an inner 90°-ply thickness below 0.4 mm and completely suppressed at 90°-ply thickness below 0.1 mm [4]. Additionally, by varying the ply thickness a change in the propagation of edge cracks is observed, with

slowly propagating cracks (slow crack growth) for thinner plies and nearly instantaneous cracks through the width (high crack growth) for thicker plies [4]. When cracks grow fast through the width, the stress is reduced, which is not fully the case for a low crack growth rate is lower. This leads to the formation of new cracks in thinner plies [5–8]. Thus, the crack distance is also a function of the ply thickness [4]. Other studies also reported a higher stress at the onset of inter fibre failure (IFF) with decreasing ply thickness [9].

With the development of thin-ply laminates by tow spreading techniques [10, 11] lower ply thicknesses in laminates can be achieved. Experimental results for carbon fibre reinforced plastic (CFRP) thin-ply laminates with a thickness of less than 50 μm show great potential in the suppression of IFF. Reducing the ply thickness leads to a delay in the onset of damage to higher tensile loads [11–13]. Saito et al. [14] investigated crack initiation and propagation in CFRP cross-ply laminates and reported, that cracks run completely through the thickness after initial failure at the fibre matrix interface for conventional prepreg plies. For thin-ply, cracks initiates in the middle but crack propagation is constrained and stress is transferred to the neighbouring layers resulting in a crack propagation through the thickness at higher strains compared to the thicker plies [14]. The damage propagation is significantly reduced in both, the width and thickness direction with decreasing the ply thickness [4, 11, 12, 14].

In this work, the influence of the 90° layer thickness on the formation of fibre matrix debonding and damage propagation as IFF in CFRP cross ply laminates is investigated micromechanically with a multi-scale approach simulation (FEM) for a range of 90°-ply thickness from 20 μm up to 190 μm . The experiments carried out focus on crack propagation in the width direction for slightly larger ply thicknesses and results are compared qualitatively with the results obtained by FE-simulation.

2. Experimental Study

2.1. Materials and sample preparation

Unidirectional prepreg material HexPly-M21/34%/UD194/T800S provided by Hexcel, with cured ply thickness of approximately 190 μm , is used for producing specimens for tension tests. The lay-up is $[0^\circ/90_n^\circ/0^\circ]$, where n is varied with $n = 1, 2, 3, 4, 8, 10$, in order to investigate the influence of the 90°-layer thickness. The specimen geometry is according to DIN EN ISO 527-4 [15] with length $l \geq 250$ mm and width $w = 25$ mm \pm 0.5 mm. As the 90°-layer thickness is varied, specimen thickness deviates from the normative reference and only the dimensions of the specimens with $n = 8$ fulfil this requirement [15]. Laminate plates of 300 mm \times 300 mm are laid-up by hand and cured with a curing cycle recommended by the manufacturer in an autoclave (curing pressure = 7 bar, temperature = 180 °C for 150 min). For regarding statistical variations of the manufacturing process within the test results, two plates of each configuration are produced. End tabs with a length of 50 mm consisting of respectively 1 mm thick GFRP and aluminium strips are glued on the plates by using a 2-component epoxy adhesive (UHU Endfest 300), leaving a distance of $l_0 = 150$ mm \pm 1 mm between the tabs. Specimens are then cut out of the laminates by using a diamond saw and are dried according to DIN EN 3615 [16] before testing in order to avoid moisture influence on the results.

2.2. Tensile tests and analysis methods

Quasi static tensile tests (DIN EN ISO 527-4 [15]) are carried out by using a Zwick/Roell Z100 universal test machine at a cross-head speed of 2 mm/min. The load is continuously measured with a load cell with a maximum load of 100 kN. The displacement is recorded via an inductive distance sensor.

The recording of acoustic emission (AE) data is carried out with a Micro-II multi-channel acquisition system from MISTRAS. Two wideband differential (WD) sensors for AE wave detection are fixed on one side of the free test length using silicone grease as coupling agent between sensor and specimen

surface. Internal filters and a static threshold are used to reduce disturbance variables, such as machine vibrations and ambient noise. The setting of the AE acquisition system is given in table 1.

In addition to tension tests until final failure, some specimens of each configuration are tested to a strain of respectively 0.2 %, 0.4 %, 0.7 % and 1.0 % and the crack development is analysed via ex-situ x-ray measurements. Zinc iodide is used as contrast medium and x-ray intensity is set to 20 keV.

Table 1. Setting of the parameters of the AE acquisition system

Parameter	Value and unit
Sampling rate	5 Mhz
Preamp gain	20 dB
Treshhold	45 dB
HDT	250 μ s
HLT	800 μ s
PDT	150 μ s

3. Test results

In the tested configurations, no significant influence of 90°-layer thickness on stiffness or tensile strength, both normalised with the thickness of the specimens to exclude geometric influences, is observed. Nonetheless, differences in damage development and final failure mode are observed. Thinner specimens with $n = 1, 2, 3$ fail in a brittle way with 0°-fibre breakage resulting in a clear crack perpendicular to the loading direction. Specimens with a larger 90°-layer thickness ($n \geq 4$) exhibit a more progressive failure mode with large delaminations and fibre splitting.

AE-analysis shows a clear trend, that damage initiates at lower strains with increasing ply thickness. First transverse cracks initiate at a strain of approximately 0.15 % for the [0°/90₈/0°] specimens and at approximately 0.45 % strain for the [0°/90°/0°] specimens. The X-ray images show that cracks perpendicular to loading direction initiate at the edges of the specimen and grow inward. Polishing of the edges increases the strain at crack initiation. The crack density, transverse cracks per length, as well as the crack length through the width depend on the 90°-layer thickness. The specimens with $n = 1$ 90°-layer have more than two time as many transverse cracks as the thickest specimens with $n = 10$ 90°-layers at strains between 0.7 % and 1.0 %. With increasing 90°-layer thickness a change in transverse crack geometry from thin, slowly growing edge cracking for thinner 90°-layer thicknesses ($n = 1, 2$) to broad cracks through the width that grow instantaneous ($n = 8, 10$) is observed. Until a strain of 1.0 %, no cracks through the width of the laminate are observed for $n = 1, 2$, whereas for $n \geq 8$ first cracks penetrating the width are observed at a strain of 0.2 %. These cracks through the width of the specimen have a larger crack opening compared to the edge cracking observed in the thinner specimens. AE-analysis and interrupted tests with X-ray images show good agreement regarding the strain at failure initiation.

4. Modelling

A finite element model is created in *Abaqus 6.14*. The model represents a cross-ply laminate with the stacking sequence [0°/90°/0°]. The 90°-layer includes the modelling of the fibre, matrix and the fibre-matrix interface, while the 0°-layer is homogenised. The fibres in the 90°-layer are distributed by using an algorithm based on the work of Melro et al. [17]. The algorithm is enhanced to recreate randomly distributed fibre diameters based on a Gaussian distribution. A fibre volume fraction of 55 % is assumed. The thickness t of the 90°-layer is varied between 20 μ m and 140 μ m, whereas the thickness of the 0°-layer is kept constant to 30 μ m for all simulations.

The homogenised 0°-layer and the fibres are discretised by eight-node continuum elements. For the matrix six-node continuum elements are used in addition because of the complex geometry. The fibre-matrix interface and the interface between the 0° and 90°-layers are represented by cohesive zone elements with a bilinear cohesive zone model. Cohesive zone elements are able to successfully recreate the fibre-matrix debonding in various micromechanical models of composites [8, 12, 18]. The material properties of the fibre and homogenized 0°-layer are summarised in table 2. Both components have linear elastic anisotropic mechanical properties.

Table 2. Material properties of the fibre and the homogenised 0°-layer in the FEM approach

Parameter	Symbol	Value and unit	
		Fibre	0°-layer
Density	ρ_{0°	1.80 g/cm ³	1.57 g/cm ³
Young's modulus (parallel)	E_{\parallel}	294 GPa	165 GPa
Young's modulus (transverse)	E_{\perp}	15 GPa	6.61 GPa
Shear modulus	$G_{\perp\parallel}$	15 GPa	4.80 GPa
Shear modulus	$G_{\perp\perp}$	7 GPa	2.75 GPa
Poissons ratio	$\nu_{\perp\parallel}$	0.2	0.28
Poissons ratio	$\nu_{\perp\perp}$	0.41	0.40

The material behaviour of the matrix is represented by an Extended Drucker-Prager material model and is extended by a damage evolution law to recreate failure. With the Extended Drucker-Prager material model different yield points for tensile, compression and shear load is achieved. Table 3 summarizes the material properties for the matrix. The input data as well as the stress-strain curve for the definition of the plasticity, given in figure 1, are part of the work of Fiedler et al. [19].

Table 3. Material properties of the matrix in the FEM approach (values from [19])

Parameter	Symbol	Value and unit
Density	ρ_M	1.28 g/cm ³
Young's modulus	E_M	3.93 GPa
Shear modulus	G_M	1.35 GPa
Poissons ratio	ν_M	0.45

The cohesive zone materials for the fibre-matrix interface and the interface between the 0° and 90°-layer require input in form of the maximum traction and the critical energy release rate. The cohesive zone material properties are summarised in table 4. The material properties used for the fibre-matrix interface are those determined by Ogihara et al. [20] and Varna et al. [21]. Considering the interface between the 0° and 90°-layer, the material properties determined by Camanho et al. [22] are used.

Symmetry boundary conditions are applied to the surfaces parallel to the symmetry planes xy and xz according to figure 2. Additionally, symmetry boundary conditions are used for the bottom surface parallel to the xz plane to ensure a statically defined state. The constant displacement u is applied to one of the surfaces parallel to the yz plane, which causes a tensile load of the cross-ply laminate. The shape change of the geometry, due to the applied load is indicated by dashed lines. A global strain of 2.0 % is applied in x-direction. The results are evaluated in steps of 0.2 % applied global strain.

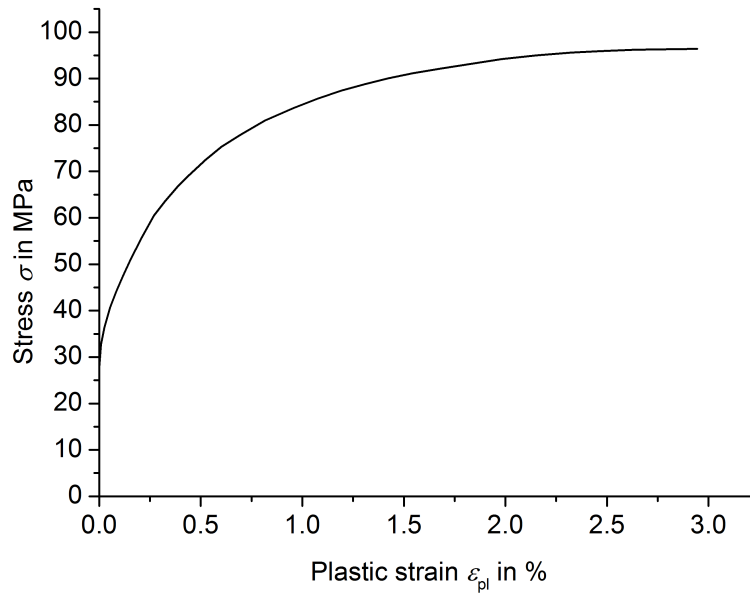


Figure 1. Stress-plastic strain hardening curve of the matrix used in the FEM approach (after [19])

Table 4. Material properties of the fibre-matrix interface and the interface between the 0° and 90°-layer in the FEM approach (values from [20–22])

Parameter	Symbol	Value and unit	
		Fibre-matrix interface	Interface between 0° and 90°-layer
Maximum Traction Mode I	T_I^{max}	50.0 MPa	93.0 MPa
Energy release rate Mode I	H_I^c	0.002 N/mm	0.277 N/mm
Maximum Traction Mode II	T_{II}^{max}	50.0 MPa	93.0 MPa
Energy release rate Mode II	H_{II}^c	0.006 N/mm	0.788 N/mm

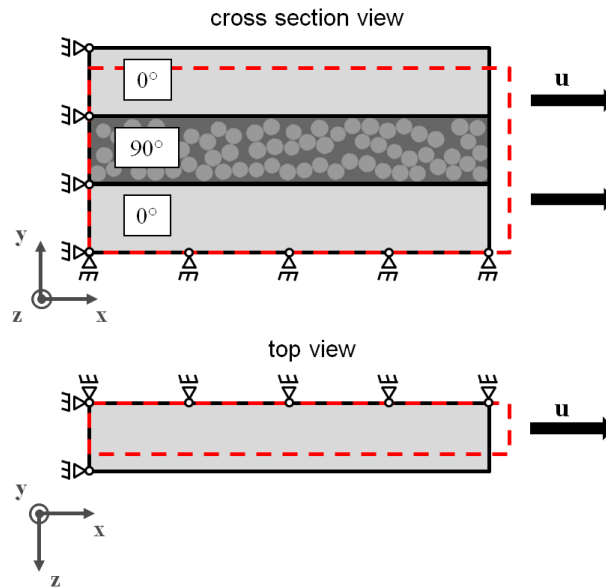


Figure 2. Boundary conditions for cross-ply laminates in the in the FE model

Figure 3 shows the equivalent stress in the 90°-layers with thickness 20 μm , 40 μm and 60 μm respectively at an applied global strain of 2.0 %. The results of the simulation show that crack distance and crack opening increase with increasing layer thickness due to stress redistribution. This stress redistribution, which takes place in the vicinity of a formed crack, results in an increasing crack distance. While all the layers have matching dimension except of the thickness, the layers with higher thickness absorb the introduced energy with less cracks, which results in larger crack openings.

Another investigated topic is the damage initiation. Therefore the reaction forces at the 90°-layer are converted to a homogenized stress and plotted during the application of the strain. The damage initiation can be seen from the drop of the homogenized stress. Figure 4 shows the applied global strain at the damage initiation for the different ply thicknesses. The damage initiation takes place at lower applied strains for an increasing ply thickness. The differences in the damage initiation seem to be significant for the different ply thicknesses. While the damage in the 140 μm layer initiates at an applied global strain of 1.00 %, damage initiation for the 20 μm layer takes place at an applied global strain of 1.35 %.

5. Discussion

No significant influence of 90°-layer thickness on stiffness and tensile strength is observed in the experiments. The 0°-layers dominate both, strength and stiffness and although scaled up by a factor of 10, the 90°-layer thickness leads to no significant change regarding final failure. In contrast, a significant change in tensile strength with decreasing ply thickness is reported in literature for thin-ply laminates with a ply thickness below 50 μm [11, 13]. With the thinnest 90°-layer thickness being 190 μm and 1900 μm , specimens tested here are in the region of conventional prepreg laminates. The mechanisms being beneficial in thin-ply laminates, such as the in-site strength [23, 24], do not apply for the tested configurations. Comparing results for thin-ply laminates with the results for high ply thicknesses, size effects due to a volume increase, based on the weakest link theory [25, 26], can be excluded as an explanation for the strength increase of thin-ply laminates.

Damage initiation is earlier for thicker plies, as reported in literature [4, 11–13]. This is shown to be valid for both, the initiation of inter-fibre fracture and cracks running through the thickness of a 90°-layer and

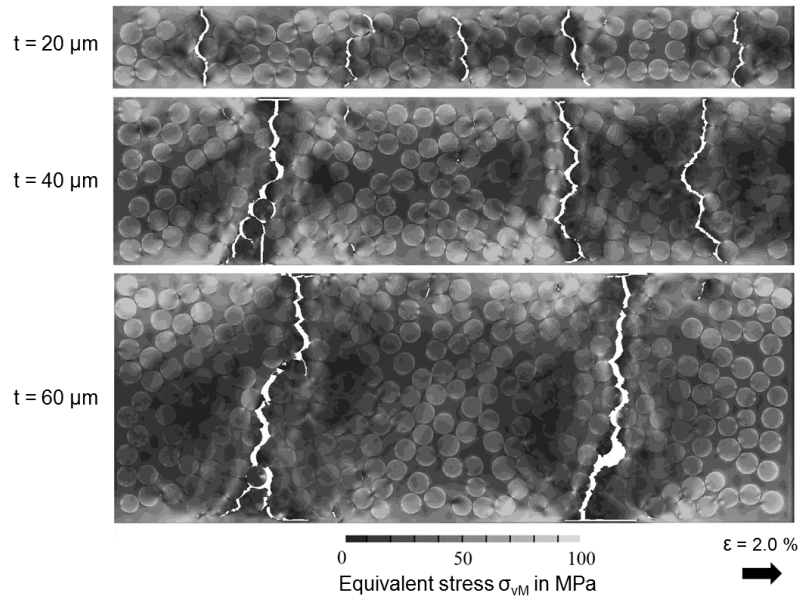


Figure 3. Equivalent stress in the 20 μm , 40 μm and 60 μm layer for an applied global strain of 2 %

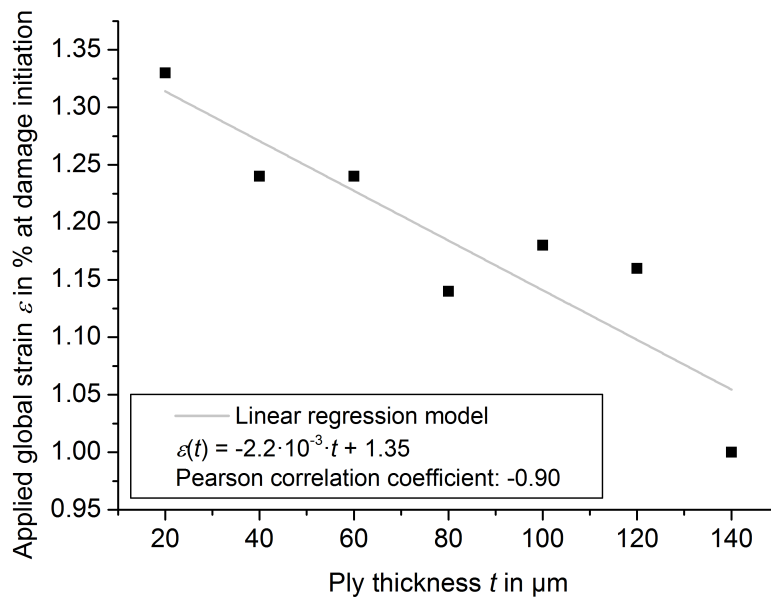


Figure 4. Global strain at damage initiation as a function of the ply thickness

transverse cracking initiating at stress concentrations at the free edges. In both cases, the crack density and crack growth rate depend on layer thickness. Regarding the crack distance, the stress redistribution at a crack through the thickness of a layer as a function of this thickness found in the simulation explains the increase in transverse crack distance with increasing layer thickness found in the experiments. A larger crack opening resulting in broader cracks with increasing layer thickness is observed for matrix crack propagation in both thickness (FEM) and width (Experiment) direction. Thus, not only damage initiation but also damage propagation and crack geometry depends strongly on the 90°-layer thickness with thinner layers offering clear advantages with regard to static or fatigue properties in tension.

AE-analysis results for strain at crack initiation show good agreement with X-ray images in interrupted tests up to defined strain levels. Therefore, with the chosen parameters, the damage state inside a cross-ply laminate can be well observed using AE-analysis.

6. Conclusion

The influence of layer thickness on failure initiation and damage propagation as matrix cracks in the 90°-layers of cross-ply laminates is investigated experimentally and with a FEM simulation. The simulation and the experiments show qualitative very good agreement. The crack density and the shape of IFF also depend on the layer thickness. With increasing 90°-layer thickness the total amount of cracks decreases, whereas the amount of cracks running through the layer thickness and through the whole specimen width increases. This case is more severe for initiating delaminations. Thus laminates with thicker layers show a more progressive delamination failure, whereas thinner layers result in a brittle failure mode. In addition, the crack growth rate is higher and cracks exhibit larger crack opening with increasing layer thickness. Damage initiates in cross-ply laminates at lower strains with increasing ply thickness. This is valid for a broad range of 90°-layer thickness from 20 µm up to 1900 µm. Tensile strength of these laminates is determined by the 0°-layers and can only be significantly increased with thin-ply but, on the other hand, does thus not decrease when increasing the thickness further, which may be of relevance, when regarding thick laminates as used in wind turbine industry. Concluding one can say that a reduction of ply thickness in cross-ply laminates increases the resistance against inter-fibre-fracture and thus offer great potential for increased fatigue lifetime.

Acknowledgments

This work was carried out with funding from the German Research Foundation (DFG) within the project number FI 688/5-1. This financial support is gratefully acknowledged.

References

- [1] C. Mittelstedt and W. Becker. Free-edge effects in composite laminates. *Applied Mechanics Reviews*, 60(5):217–245, 2007.
- [2] T. Okabe, H. Imamura, Y. Sato, R. Higuchi, J. Koyanagi, and R. Talreja. Experimental and numerical studies of initial cracking in CFRP cross-ply laminates. *Composites Part A: Applied Science and Manufacturing*, 68:81–89, 2015.
- [3] Isaac M. Daniel and Ori Ishai. *Engineering mechanics of composite materials*. Oxford University Press, New York, 1994.
- [4] A. Parvizi, K. W. Garrett, and J. E. Bailey. Constrained cracking in glass fibre-reinforced epoxy cross-ply laminates. *Journal of Materials Science*, 13(1):195–201, 1978.

- [5] A. Parvizi and J. E. Bailey. On multiple transverse cracking in glass fibre epoxy cross-ply laminates. *Journal of Materials Science*, 13(10):2131–2136, 1978.
- [6] J. E. Bailey, P. T. Curtis, and A. Parvizi. On the transverse cracking and longitudinal splitting behaviour of glass and carbon fibre reinforced epoxy cross ply laminates and the effect of poisson and thermally generated strain. *Proceedings of the Royal Society of London A: Mathematical, Physical and Engineering Sciences*, 366(1727):599–623, 1979.
- [7] T. Yokozeki, T. Aoki, and T. Ishikawa. Transverse Crack Propagation in the Specimen Width Direction of CFRP Laminates under Static Tensile Loadings. *Journal of Composite Materials*, 36(17):2085–2099, 2002.
- [8] A. Arteiro, G. Catalanotti, A. R. Melro, P. Linde, and Pedro P. Camanho. Micro-mechanical analysis of the in situ effect in polymer composite laminates. *Composite Structures*, 116(0):827–840, 2014.
- [9] H. Saito, M. Morita, K. Kawabe, M. Kanasaki, H. Takeuchi, M. Tanaka, and I. Kimpara. Effect of ply-thickness on impact damage morphology in cfrp laminates. *Journal of Reinforced Plastics and Composites*, 30(13):1097–1106, 2011.
- [10] S. W. Tsai, S. Sihm, and R. Y. Kim. Thin ply composites. In *46th AIAA/ASME/ASCE/AHS/ASC Structures 2005, Structural Dynamics & Materials Conference*. American Institute of Aeronautics and Astronautics, Austin and Texas and USA, 2005.
- [11] S. Sihm, R. Y. Kim, K. Kawabe, and S. W. Tsai. Experimental studies of thin-ply laminated composites. *Composites Science and Technology*, 67(6):996–1008, 2007.
- [12] H. Saito, H. Takeuchi, and I. Kimpara. A study of crack suppression mechanism of thin-ply carbon-fiber-reinforced polymer laminate with mesoscopic numerical simulation. *Journal of Composite Materials*, 48(17):2085–2096, 2014.
- [13] R. Amacher, J. Cugnoni, J. Botsis, L. Sorensen, W. Smith, and C. Dransfeld. Thin ply composites: Experimental characterization and modeling of size-effects. *Composites Science and Technology*, 101(0):121–132, 2014.
- [14] H. Saito, H. Takeuchi, and I. Kimpara. Experimental Evaluation of the Damage Growth Restraining in 90 Layer of Thin-ply CFRP Cross-ply Laminates. *Advanced Composite Materials*, 21(1):57–66, 2012.
- [15] Deutsches Institut für Normung e.V. Plastics - Determination of tensile properties - Part 4: Test conditions for isotropic and anisotropic fibre-reinforced plastic composites, 1997. DIN EN ISO 527-4.
- [16] Deutsches Institut für Normung e.V. Aerospace series; fibre reinforced plastics; determination of the conditions of exposure to humid atmosphere and of moisture absorption, 1999. DIN EN 3615.
- [17] A. Melro, P. Camanho, and S. Pinho. Generation of random distribution of fibres in long-fibre reinforced composites. *Composites Science and Technology*, 68(9):2092–2102, 2008.
- [18] J. Koyanagi, P. D. Shah, S. Kimura, S.K. Ha, and H. Kawada. Mixed-mode interfacial debonding simulation in single-fiber composite under a transverse load. *Journal of Solid Mechanics and Materials Engineering*, 3(5):796–806, 2009.
- [19] B. Fiedler, M. Hojo, S. Ochiai, K. Schulte, and M. Ando. Failure behavior of an epoxy matrix under different kinds of static loading. *Composites Science and Technology*, 61(11):1615–1624, 2001.

- [20] S. Ogihara, Y. Sakamoto, and J. Koyanagi. Evaluation of interfacial tensile strength in glass fiber/epoxy resin interface using the cruciform specimen method. *Journal of Solid Mechanics and Materials Engineering*, 3(9):1071–1080, 2009.
- [21] J. Varna, L.A. Berglund, and M.L. Ericson. Transverse single-fibre test for interfacial debonding in composites: 2. modelling. *Composites Part A: Applied Science and Manufacturing*, 28(4):317–326, 1997.
- [22] P. P. Camanho, P. Maimí, and C. G. Dávila. Prediction of size effects in notched laminates using continuum damage mechanics. *Composites Science and Technology*, 67(13):2715–2727, 2007.
- [23] D. L. Flagg and M. H. Kural. Experimental determination of the in situ transverse lamina strength in graphite/epoxy laminates. *Journal of Composite Materials*, 16(2):103–116, 1982.
- [24] P. P. Camanho, C. G. Dávila, S. T. Pinho, L. Iannucci, and P. Robinson. Prediction of in situ strengths and matrix cracking in composites under transverse tension and in-plane shear. *CompTest* 2004, 37(2):165–176, 2006.
- [25] W Weibull. A statistical theory of the strength of materials. *Royal Swedish Institute Engineering Research*, 151:1–45, 1939.
- [26] W Weibull. A statistical distribution function of wide applicability. *Journal of Applied Mechancis*, 18:293–29, 1951.